JASMAC
Conference of the Japan Society of Microgravity Application

PS10

DEM 解析における月模擬砂 FJS-1 の力学挙動再現を目的とした粒子モデル作成と校正

Creation and Calibration of a Particle Models for Reproducing the Mechanical Behavior of Lunar Soil Simulant FJS-1 in DEM Analysis

松尾昂輝 [1], 梶原健生 [2], 渡辺公貴 [2], 川口正隆 [2], 田中和人 [2]
[1] 同志社大学大学院，Graduate School of life and Medical Science Doshisha
[2] 同志社大学，Doshisha University

1. Introdction

The soft ground composed of fine particles called regolith on the lunar surface poses obstacles such as slippage and getting stuck for rovers during traversal[1)]. Therefore, understanding the mechanical properties of lunar soil and predicting and evaluating the traversal performance of rovers are crucial for establishing future mobility technologies. The Discrete Element Method (DEM) numerical simulation is expected to be useful due to its ability to visualize the interaction between sand and wheels exhibiting nonlinear movements and consider in-situ factors such as low-gravity environments. In DEM analysis for evaluating the traversal performance of rovers, spherical elements are generally used for soil particles from the perspective of contact detection and computational speed. However, it has been revealed that the particle size distribution and particle shape of irregular powder materials like regolith significantly influence the mechanical properties of the powder[2)]. In this study, to reproduce the mechanical behavior of the lunar simulant sand FJS-1 in DEM analysis, we constructed a particle model based on three-dimensional observations using X-ray CT and calibrated DEM parameters through angle of repose experiments.

2. DEM methodology and calibration approach

2.1. X-ray CT measurement and particle modelling.

In soil mechanics, it is known that parameters such as particle shape, size distribution, and porosity have significant effects on the mechanical properties of the soil[2)]. This experiment aimed to model and simulate the irregular particle shapes of the lunar simulant sand FJS-1[3)]. We measured the 3D shapes of the particles by using a high-resolution 3D X-ray microscope (Rigaku Corporation, nano3DX). The 3D particle images obtained from the observations are shown in Figure 1. For each particle shown in Figure 1, a bounding box as shown in Figure 2 was constructed, and the dimensions of each side were defined as a, b, and c. When setting the conditions $a \le b \le c$, the bounding box in Figure 2 can be divided into four cases. Based on these four cases, the particle shapes were classified into the four shapes shown in Figure 3, and particle models were created. In creating the particle models, the arrangement of spherical elements in each model was made to satisfy the conditions (i) ~ (iv) below.

i. The four particle models are respectively composed of spherical elements with the same diameter.

ii. The spherical elements in each model should be arranged to match the average packing density of the particles within the bounding box.

iii. The particles are arranged to be inscribed within a bounding rectangular box.

iv. The number of sphere elements that make up the particle model should be set to a minimum.

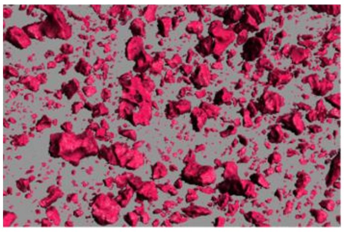

Figure 1. The 3D image of FJS-1 Particles.

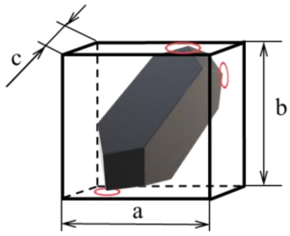

Figure 2. Bounding box circumscribed to particles.

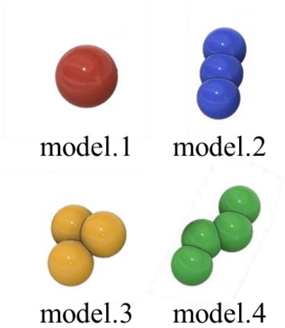

Figure 3. Particle models of lunar soil simulant.

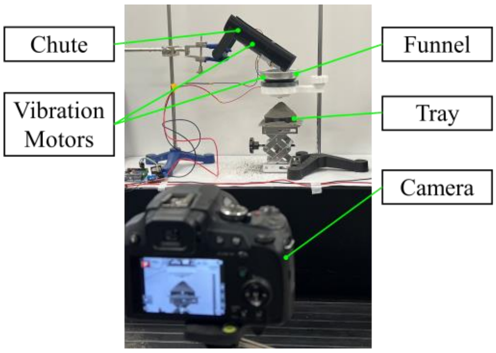

Figure 4. AoR measurement experiment.

2.2. Measurement of AoR

The angle of repose (AoR) is a fundamental indicator used to evaluate the mechanical properties of granular materials and has been widely utilized for calibrating DEM parameters. An overview of the AoR measurement experiment is shown in Figure 4. At the start of the experiment, the lunar simulant soil discharged into the tray below funnel and accumulates in a conical shape. The funnel bottom was kept within 5 mm of the lunar soil simulant tip during the experiment to reduce the impact of particle falling speed on the AoR. Additionally, a vibrating motor with speed control was used to impart a 100 Hz micro-vibration to the funnel and slide, preventing the adhesion of the simulant sand to these apparatus surfaces. Furthermore, a mesh with a size of 1.0 mm × 1.0 mm was set on the top of the funnel to exclude particles with an equivalent diameter of 1.0 mm or greater that were not DEM analysis. Under these conditions, the AoR was measured five times. After the experiment, images of the deposited simulant soil were captured with a camera positioned horizontally relative to the funnel. The images were binarized as shown in Figure 5, and edge detection was performed to delineate the surface profile without losing its roughness. The two-dimensional coordinates of the divided lines were calculated, and the AoR was determined.

$$\phi_r = \tan^{-1} a \tag{1}$$

From equation (1), the angle of repose obtained in this experiment was 40.9 ± 1.17°.

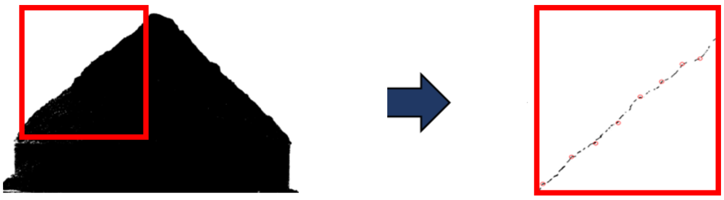

(a) Binary image of the deposited FJS-1. (b) Edge-detected image.

Figure 5. Method of calculating AoR.

2.3. Calibration of the DEM parameters of lunar soil simulant

The fluid analysis software Ansys Rocky 2023 R.1.1 was used to simulate the angle of repose measurement. Among the many parameters to be input to the simulation, it has been reported that the static and rolling friction coefficients have a high contribution to the angle of repose[5]. Therefore, in this research, simulation was calibrated by matching the experimental values of the angle of repose with the analytical response, using as variables the static friction coefficient μ_1 and the rolling friction coefficient μ_2 of the particles, which are considered difficult to measure directly. The employed apparatus for measuring the AoR in the simulation is shown in Fig. 6. The particle model used was the described in section 2.1. The particle size and shape distributions of the model are shown in Figure 7. Other parameters used in the simulation are listed in Table 1 below. Considering that FJS-1 particles have adhesive properties, a model combining the contact theory of Hertz-Mindlin with the adhesion theory of JKR was used as the contact model in this simulation[6].

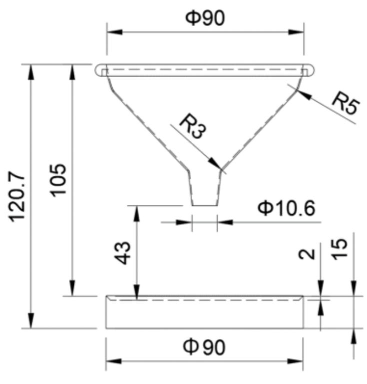

Figure 6. The employed apparatus for measuring the AoR in simulation.

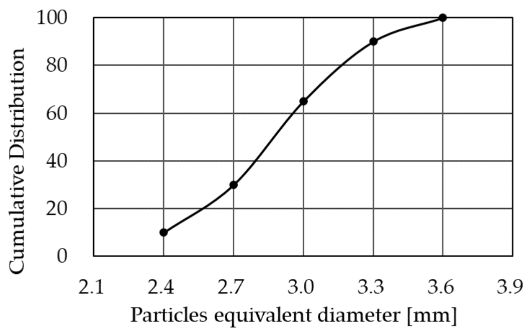

Figure 7. Particle size distribution in simulation.

Table 1. Material parameters in DEM simulation.

Parameter	Value
Bulk density of lunar soil simulant [kg/m^3]	1360
Young's modulus of lunar soil simulant [MPa]	42.5
Poisson's ratio of lunar soil simulant	0.25
Inner restitution coefficient of lunar soil simulant	0.5
Inner static friction coefficient of lunar soil simulant	0.2 - 0.4
Inner rolling friction coefficient of lunar soil simulant	0.01 - 0.15
Surface energy for lunar soil simulant [J/m2]	0.01

3. Results

3.1. Effect of static and rolling friction coefficients on AoR

As shown in Table 1, the static friction coefficient μ_1 was varied from 0.2 to 0.5 in 0.1 increments and the rolling friction coefficient μ_2 was varied from 0.01 to 0.15 in 0.07 increments for a total of 9 simulations. The results are shown in Figure 8. A comparison of simulated and experimental AoR is shown in Figure 9.

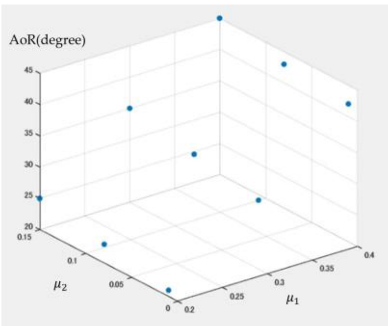

Figure 8. interaction effect of μ1 and μ2 on AoR

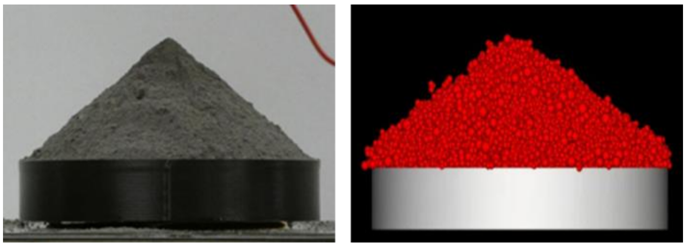

Figure 9. Comparison of simulated and experimental AoR.

In Figure 8, the larger the static friction coefficient μ_1 is, the higher the value of the AoR is for the larger rolling friction coefficient μ_2. Figure9 shows that at (μ_1, μ_2) = (0.4, 0.01), the AoR is 41.1°, which is the closest value to the experimental result. Based on this result, multiple regression analysis was conducted with AoR as the dependent variable and μ_1 and μ_2 as independent variables. The regression equation can be expressed as Equation (2) below.

$$AoR = 103\mu_1 + 25.4762\mu_2 + 0.2619 \tag{2}$$

From Equation (2), it can be observed that the contribution of μ_1 to the angle of repose is higher compared to μ_2.

3.2. Effect of the gravity acceleration on AoR

To investigate the effect of gravity on AoR, three DEM simulations under varying gravity conditions of 1/6 G and 1 G were performed. The parameters used in these simulations were the same as the optimal solutions of the regression model except the gravity acceleration. Results are shown in Figure 10.

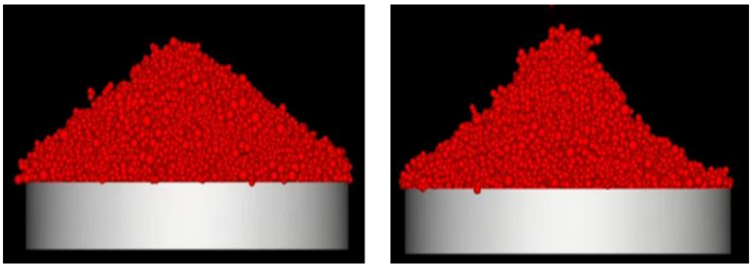

(a) 1 G. (b) 1/6G.

Figure 10. Comparison AoR for varying gravity conditions

As you can see in Figure 10, the results demonstrated that the AoR is higher at lower gravity.

4. Conclusion

This study aimed to reproduce the mechanical behavior of the lunar soil simulant FJS-1, which has irregular particle shape, and revealed that it can be calibrated by creating a particle model other than spherical elements and varying two coefficients, which are the static friction coefficient and the rolling friction coefficient. The accurate setting of DEM input parameters for the lunar soil simulant by calibration is expected to clarify the interaction between the lunar simulant sand and rover wheels in DEM analyses for future lunar exploration, and to be applied to the prediction of rover running performance.

References

1) 飯塚浩二郎, 久保田孝: 軟弱地盤走行のための月面探査ローバ用走行系検証, 科学・技術研究, Vol.**1**[1] (2012), pp.49-55. DOI: https://doi.org/10.11425/sst.1.49
2) Xuyan X, et al, : Constitutive properties of irregularly shaped lunar soil simulant particles, Powder Technology, Vol.**346** (2019), pp.137-149. DOI: https://doi.org/10.1016/j.powtec.2019.02.012
3) Kanamori, H., et al. : Properties of Lunar Soil Simulant Manufactured in Japan, Space 98, Proceedings of the Sixth International Conference and Exposition on Engineering, Construction, and Operations in Space, Galloway, R.G. and Lokaj, S. Eds. ASCE, (1998). pp. 462–468. DOI: https://doi.org/10.1061/40339(206)5
4) Thomas R, et al. : DEM parameter calibration of cohesive bulk materials using a simple angle of repose test, Particuology, Vol.**45** (2019), pp.105-115. DOI: https://doi.org/10.1016/j.partic.2018.08.005
5) Jianzhong Z, et al. : Measurement and calibration of DEM parameters of lunar soil simulant, Acta Astronautica, Vol.**191** (2022), pp.169-177. DOI: https://doi.org/10.1016/j.actaastro.2021.11.009Get rights and content
6) Mahmoud A, et al. : Theories and Applications of CFD–DEM Coupling Approach for Granular Flow: A Review, Archives of Computational Methods in Engineering, Vol.**28** (2021), pp.4979-5020. DOI: https://doi.org/10.1007/s11831-021-09568-9

© 2024 by the authors. Submitted for possible open access publication under the terms and conditions of the Creative Commons Attribution (CC BY) license (http://creativecommons.org/li censes/by/4.0/).